J Geophys (1985) 56:51–58

Journal of Geophysics

# Measurement of magnetic susceptibility anisotropy in Buntsandstein deposits from southern Germany

**Thomas Schultz-Krutisch**[1] **and Friedrich Heller**[2]

[1] Institut für Geologie, Universität Würzburg, Pleicherwall 1, D-8700 Würzburg, Federal Republic of Germany
[2] Institut für Geophysik, ETH Zürich, CH-8093 Zürich, Switzerland

**Abstract.** The anisotropy of magnetic low-field susceptibility in the Triassic Plattensandstein formation (Upper Buntsandstein) from northern Bavaria has a typical sedimentary fabric. The anisotropy ellipsoids are strongly oblate with minimum susceptibility axes normal to sedimentary bedding. The directions of the maximum susceptibility axes are consistent with the NNE-NE-trending general sediment transport direction that is derived from geological field observations of cross-bedding structures in the sandstones. However, the very small intensity differences between maximum and intermediate susceptibility require extremely sensitive mearuement techniques. Comparative measurements were made with a spinner magnetometer, a cryogenic magnetometer and a susceptibility bridge. Directionally, the most consistent results were obtained with the spinner magnetometer after it was stabilized by means of a low-pass active filter. The directional consistency of the anisotropy principal axes can be improved further by annealing the sandstones at 750° C in air. During this treatment a strongly magnetic, low-coercivity mineral phase – probably magnetite – is formed which enhances the degree of magnetic anisotropy as well as the bulk susceptibility. Low temperature measurements indicate that, in the natural unheated state, paramagnetic minerals contribute substantially to the low-field susceptibility of the sandstones at room temperature.

**Key words:** Rock magnetism – Low-field susceptibility – Anisotropy – Triassic red beds – Southern Germany

## Geological introduction

For the past 50 years cross-bedding analysis has been one of the sedimentologist's tools to delineate transport directions in sandstones (cf. Wurster, 1958). Cross-bedding structures are generated by continual development of sediment fore-casts. In this process, sand bars in fluviatile deposits progress in the current direction when sediment is deposited on the lee side of the sand bars so that the sediment strata dip very gently along the current direction. This direction can be derived from field measurements of the azimuth and dip of the bedding planes.

The Plattensandstein member of the Upper Buntsandstein formation in northwestern Bavaria is a typical cross-bedded fluviatile sediment in which palaeocurrent directions have been studied previously (Vossmerbäumer et al., 1979; Teyssen and Vossmerbäumer, 1980). The sandstone sequence is about 30–40 m thick and consists of red, partly violet, well-stratified and well-sorted fine sandstones. In a few zones the sediments are not oxidized and therefore green coloured. Silt and clay layers of up to 15-cm thickness are interbedded with the sandstones. Horizontal bedding, platy and especially trough-like cross-bedding structures are the dominant types of stratification. The trough channels have concave basal planes which cut across silt- or clay-horizons.

In an outcrop at Dietenhan, near the town of Würzburg, where the uppermost 12–15 m of the Plattensandstein have been quarried, the channels are up to 4 m wide and 1 m thick (Fig. 1). In the lower part they are bedded parallel to the slightly inclined base, in the upper part the bedding sometimes changes to the horizontal. Some channels are filled asymmetrically. Multiple cross-cutting of different channels indicates positional changes of the river. Some channels were developed at the same time, probably due to a braided river system (Allen, 1965) during the Plattensandstein sedimentation. Additional sedimentary textures are oscillation ripple marks (with irregularly divided ridges), flute casts, current crescents and sporadically load casts.

The measured cross-bedding values (Fig. 1) have been taken from all accessible cross-bedded strata at Dietenhan. In order to resolve variable strike and dip of the cross-bedded layers, each layer was measured several times, if possible. The direction of sediment transport was calculated from field measurements of the dip azimuth of the foresets following the method developed by Wurster (1958). The observations of the dip azimuth on both flanks of the cross-bedded layers result in a bimodal distribution (Fig. 2b). The vectorial mean value of the bedding poles dips steeply towards SSW with a circular standard deviation ($\psi 63$) of 10°. From this value, the local palaeocurrent direction pointing towards N18°E is derived. The dip of the cross-bedded layers is always low, especially towards the core of the channels and averages about 11° (Fig. 2a). This value is typical for through-like cross-bedding lamination.

The small dip angles and the often recognized horizontal bedding (Fig. 1) in the Plattensandstein formation make field measurements with a compass tedious, inaccurate or in some situations impossible. Thus the determination of the resulting mean current direction (Fig. 2) is strongly influenced by the quality of the measuring points as well as by their distribution which may be limited due to outcrop

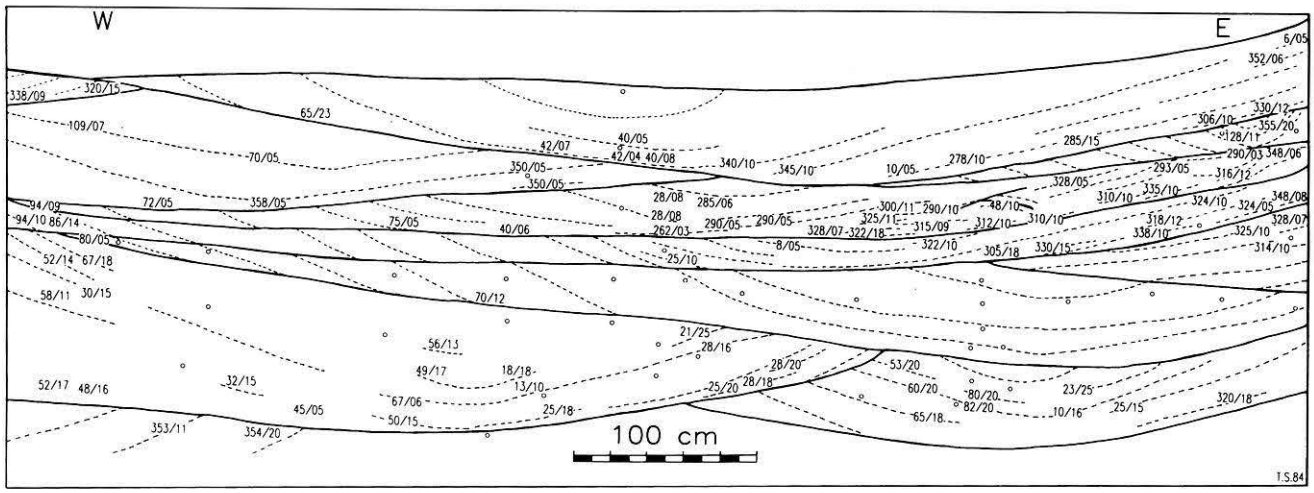


**Fig. 1.** Lithostratigraphic section of the Plattensandstein member at Dietenhan. *Solid lines:* boundaries of cross-bedded bodies; *dashed lines:* traces of bedding planes; *circles*: drill holes; *numbers* denote azimuth and dip of cross-bedding

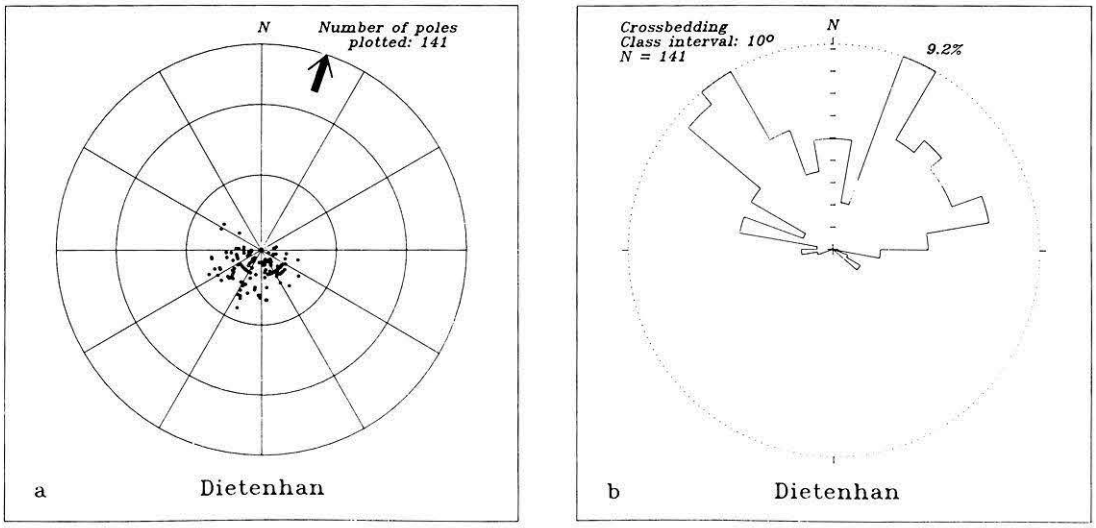


**Fig. 2. a** Orientation of cross-lamination foreset poles on equal area projection (lower hemisphere). The angular standard deviation ($\psi 63$) of the mean pole amounts to 10°. — *Arrow* represents resulting current direction to the NNE. **b** Rose diagram of the dip azimuth of cross-lamination foresets. Bimodal distribution is caused by the E and W dipping cross-bedding structures (cf. Fig. 1)

conditions. Even worse, it may be erroneous due to subjective selection criteria.

Undeformed sedimentary rocks have a magnetic fabric which is due to forces acting during and after deposition. Therefore, ancient current directions may be determined precisely by the measurement of magnetic susceptibility anisotropy (Rees, 1965). This paper describes magnetic measurement and analysis techniques applicable to the weak magnetic fabrics of red sandstones. We have drilled 40 oriented mini cores in the various sedimentary structures at Dietenhan (Fig. 1). In addition, two other nearby outcrops have been sampled, but most of the results presented in this paper refer to samples from the main quarry at Dietenhan. The cores have a diameter of 2.54 cm and are up to 10 cm long so that up to four specimens of 2.25-cm length can be cut from the same core. The length-to-diameter ratio has been chosen in order to avoid anisotropies arising from the shape of the specimens (Scriba and Heller, 1978).

## Magnetic mineralogy of the Plattensandstein

The magnetic mineralogy of red sandstones is usually dominated by haematite which occurs either as specularite or as pigmentary grain aggregations (Turner, 1980). Microscopic observations of Plattensandstein polished sections indicate specular haematite to be the major ferromagnetic constituent with negligible additional amounts of ilmenohaematite (with ilmenite exsolutions) and of unexsolved ilmenite.

The ferromagnetic minerals of the sandstones may also be identified from the analysis of the coercivity and blocking temperature characteristics of isothermal remanent magnetization (Dunlop, 1972). The shape of IRM acquisition curves and the fact that IRM is far from saturation in a 1 T field, indicates a high coercivity mineral as the main carrier of remanence (Fig. 3, Type I). Low coercivity phases are largely absent. Stepwise thermal demagnetiza-

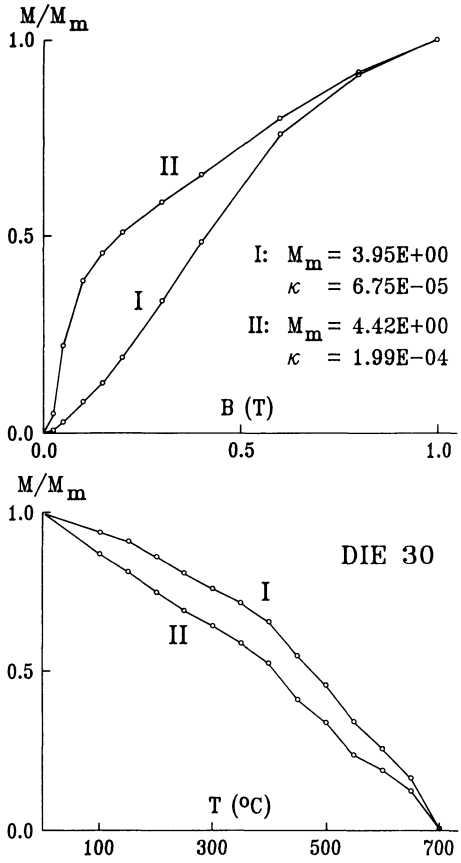


**Fig. 3.** IRM acquisition and subsequent progressive thermal demagnetization of sandstone samples in the natural state (I) and after annealing at 750° C (II). $M_m$ denotes maximum IRM [A/m], $k$ is the low-field bulk susceptibility [SI-units/cm$^3$] before thermal demagnetization

tion of IRM shows maximum unblocking temperatures above 650° C which, together with the high coercivity, indicate haematite as the main ferromagnetic mineral.

When the sandstones are annealed in air at 750° C for one hour, the magnetic properties are altered drastically (Fig. 3, Type II). A low coercivity phase with maximum unblocking temperatures around 550° C is created. Following Stephenson (1967), who performed similar heating experiments with Old Red sandstones, we tentatively ascribe this phase to magnetite. The magnetite is responsible for the strongly increased bulk susceptibility (Fig. 3) after heating. The maximum IRM intensities at room temperature, however, have nearly the same values whether heated or not. At liquid nitrogen temperature, the IRM intensities of the heated samples are up to twice as strong as the room temperature IRM. This suggests that most of the magnetite formed during annealing is superparamagnetic at room temperature. For unheated sandstones, IRMs at liquid nitrogen temperature and at room temperature are not appreciably different, which indicates an absence of superparamagnetic mineral phases and, therefore, negligible superparamagnetic contributions to the low-field susceptibility of the sandstones in the natural state.

The source of the low-field susceptibility in red sediments is often ambiguous (Collinson, 1965). In addition to ferromagnetic sources, paramagnetic and diamagnetic components may be important. Collinson (1968) and Shive et al. (1984) have shown by means of high-field experiments that the induced magnetization of red beds can be controlled by substantial amounts of paramagnetic material such as iron-rich clays, phyllosilicates and ilmenite.

The temperature dependence of the low-field susceptibility may give some information about the magnetic state of the minerals causing the measured susceptibility signal. The following technique was used to measure the susceptibility at variable temperature between liquid nitrogen and room temperature. A small-sized (4 cm$^3$) cylindrical sandstone sample was put into a styrofoam box and cooled down to liquid nitrogen temperature. Then the sample was taken out of the liquid nitrogen and allowed to warm up slowly. Its susceptibility was measured at regular time intervals with a KLY-1 susceptibility bridge. After 75 min the sample reached room temperature. The temperature calibration was performed independently in the same manner with the sample outside the susceptibility bridge, since the susceptibility of any thermocouple would completely overshadow the weak susceptibility signal of a sandstone sample.

The temperature dependence of low-field susceptibility and its reciprocal have been plotted in Fig. 4 for two unheated sandstones. The samples are dominated by paramagnetic mineral contributions which lead to a linear increase of the reciprocal susceptibility between 77 K and 250 K. Towards room temperature, non-paramagnetic mineral phases become of greater importance resulting in a non-linear reciprocal susceptibility curve. However, the extrapolated linear regression segments intercept the temperature axis at negative values. These negative Néel points, at first inspection, are suggestive of antiferromagnetic ilmenite which has a Néel temperature around −210° C. An ilmenite content (bulk susceptibility value from Bleil and Petersen 1982) of more than 1% by volume would be needed for the observed signal. However, such an amount of ilmenite is incompatible with the microscopic evidence. Microscopic examination showed that biotite, clinochlore and traces of ilmenite are present in these Plattensandstein samples. We prefer an interpretation which assigns the paramagnetic susceptibility to the biotite and clinochlore. Since the basal planes of the biotite crystals lie within the bedding planes, they may indeed be responsible for a "detritic" anisotropy.

If the amount of ilmenite, as suggested by the optical examination, is negligible and if the ferromagnetic susceptibility can be represented as temperature-independent constant between liquid nitrogen and room temperature, then an approximate estimate can be made (Table 1) about the contributions of diamagnetic, paramagnetic and ferromagnetic minerals to the measured susceptibility. Since diamagnetic minerals such as quartz and feldspar make up nearly 100% of the sandstones, a constant diamagnetic value can be added to the measured bulk susceptibility. A rough estimate of the ferromagnetic susceptibility is then obtained by shifting the signal until the regression line hits the origin of the temperature axis.

In both samples the paramagnetic minerals predominate over the other two contributions (Table 1). The ferromagnetic susceptibility of sample DIE38A is about 45% higher than that of the sample WES02B. It is interesting to note that the same relation holds for the IRM intensities (Table 1) and thus confirms the derivation of a higher content of ferromagnetic minerals, i.e. of haematite, in sample DIE38A.

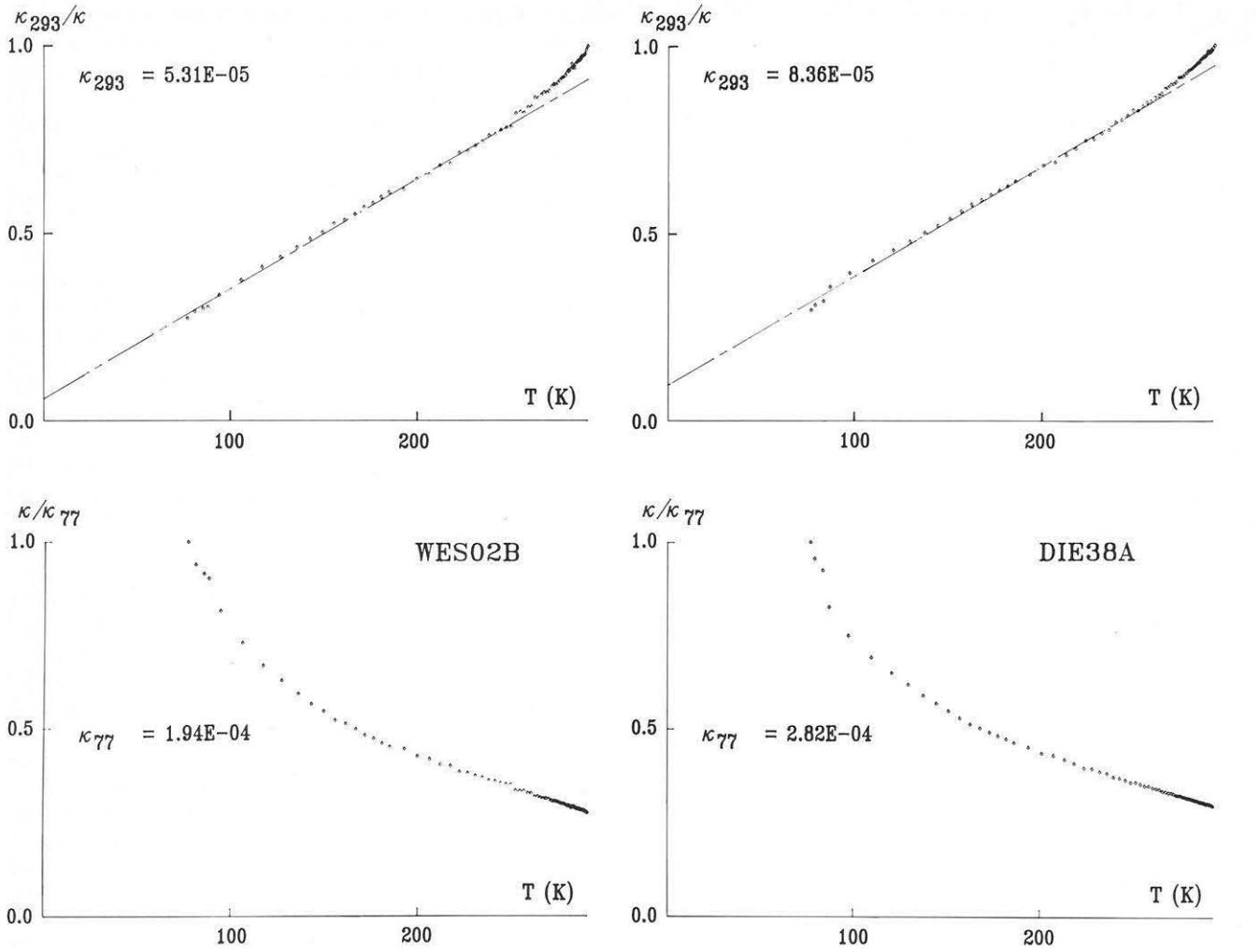


**Fig. 4.** Temperature dependence of low-field susceptibility and reciprocal of low-field susceptibility for two unheated red sandstone samples. Regression lines were computed between 77 K and 250 K. Values in SI-units/cm$^3$

**Table 1.** Estimates of paramagnetic, diamagnetic and ferromagnetic susceptibility contributions and IRM intensity (acquired in a 1 Tesla field) of two unheated sandstone samples

| Sample | Susceptibility [SI-units/cc] | | | | IRM [A/m] |
|---|---|---|---|---|---|
| | Measured | Paramagnetic | Diamagnetic | Ferromagnetic | |
| DIE38A | 8.36E-05 | 5.69E-05 | −1.53E-05 | 4.20E-05 | 2.02 |
| WES02B | 5.31E-05 | 4.09E-05 | −1.53E-05 | 2.83E-05 | 1.41 |

## Magnetic susceptibility anisotropy

The magnetization ($\mathbf{M}_i$) of a sample which is placed in a magnetic field $\mathbf{H}_i$ can be characterized by

$$\mathbf{M}_i = k_{ij}\,\mathbf{H}_i$$

with the susceptibility $k_{ij}$ being a tensor of the second order, which can be described geometrically as an ellipsoid with the three principal axes $k_{max}$, $k_{int}$ and $k_{min}$. The degree of anisotropy is often expressed by the ratios of the intensities of the principal axes,

$P_1 = k_{max}/k_{min}$,
$P_2 = k_{max}/k_{int}$,
$P_3 = k_{int}/k_{min}$.

Ising (1942) established that the minimum axes of the anisotropy ellipsoid in Swedish varved clays are oriented perpendicular to the bedding planes. Various natural and laboratory produced depositional sedimentary fabrics were investigated by Rees (1961, 1965, 1968), Rees et al. (1968), Hamilton (1967) and Hamilton and Rees (1971) measuring magnetic susceptibility anisotropy. Generally, the orientation of magnetic particles depends on the earth's gravity field, the strength of the depositing current, the dip of the bedding plane, the shape of a sediment particle and the strength and direction of the geomagnetic field (Hamilton et al., 1968). The laboratory experiments of these authors proved that gravity and hydrodynamic forces are much more efficient than the influence of the geomagnetic field for the particle settling in fine grained sandstones. They

**Table 2.** Anisotropy data obtained by different measuring techniques

| Instrument | $k_{max}$ | | | | $k_{min}$ | | | | $P_1$ | $P_2$ | Susc. | $N$ |
|---|---|---|---|---|---|---|---|---|---|---|---|---|
| | Az | Dip | $\psi_{63}$ | $k$ | Az | Dip | $\psi_{63}$ | $k$ | | | | |
| Digico without filter | 0.6 | −1.7 | 34.9 | 5.4 | 107.7 | 87.7 | 13.7 | 34.8 | 1.068 | 1.014 | 6.309 | 69 |
| Digico with filter | 46.8 | 1.0 | 28.6 | 8.0 | 185.8 | 89.0 | 9.1 | 79.7 | 1.050 | 1.009 | 6.335 | 69 |
| ScT | 21.6 | 3.4 | 41.5 | 3.8 | 223.0 | 85.3 | 8.7 | 86.7 | 1.055 | 1.007 | 6.211 | 69 |
| KLY-1 manual | 54.2 | 0.8 | 48.5 | 2.8 | 338.1 | 83.8 | 7.8 | 107.3 | 1.054 | 1.008 | 5.315 | 8 |
| KLY-1 on-line | 27.8 | 4.9 | 33.3 | 5.9 | 356.6 | 84.7 | 5.4 | 221.4 | 1.050 | 1.006 | 5.128 | 8 |
| Digico with filter | 39.8 | 2.7 | 24.9 | 10.6 | 352.8 | 87.6 | 6.4 | 162.0 | 1.044 | 1.006 | 6.119 | 8 |
| Digico unheated | 42.0 | 1.3 | 21.8 | 13.8 | 248.5 | 88.9 | 9.8 | 68.5 | 1.050 | 1.009 | 6.583 | 39 |
| Digico heated | 38.5 | 0.6 | 18.9 | 18.4 | 200.3 | 89.2 | 7.6 | 113.5 | 1.192 | 1.025 | 19.280 | 42 |

Azimuth (Az) and dip of $k_{max}$ and $k_{min}$ mean directions with circular standard deviation ($\psi 63$) and Fisher (1953) precision parameter ($k$). Mean volume susceptibilities (Susc.) in SI-units/$10^{-5}$ from $N$ samples

produce preferential alignment of grain short axes normal to bedding and grain long axes parallel to current flow.

The relation between palaeocurrent directions and susceptibility anisotropy in different types of undeformed sandstones has been investigated by several authors (Crimes and Oldershaw, 1967; Galehouse, 1968; Rad, 1970; Hrouda and Janak, 1971; Hamilton and Rees, 1971; Argenton et al., 1975; Van den Ende, 1975; Channell et al., 1979). Hrouda and Janak (1971) found that $P_2$ factors were always very low ($1.0 < P_2 < 1.01$) in red sandstones. The maximum anisotropy directions were often poorly defined, but generally were oriented parallel to sedimentological features such as cross-bedding foresets, ripple marks or flute casts (Rad, 1970). According to Hrouda and Janak (1971), the $P_3$ factors are always higher than $P_2$ ($P_3 > 1.01$), representing an anisotropy to be expected for a sedimentary or compaction texture. On the other hand, in Permian red sandstones where the magnetic fabric was thought to be caused by the alignment of platy haematite crystals, Van den Ende (1975) found that the maximum axes of susceptibility were oriented perpendicular to the current direction markers and great circle distributions of these axes could often not be interpreted.

The differences amongst these observations and the poor definition of the orientation of maximum anisotropy axes may result partly from inaccurate measuring methods. Therefore, when measuring the Plattensandstein magnetic fabric, several magnetometers and different measurement techniques were applied and tested.

## Different techniques for magnetic anisotropy measurement of Plattensandstein samples

1. The Digico spinner magnetometer measures relative susceptibility differences in three orthogonal planes of a sample. To get the absolute anisotropy values, the axial bulk susceptibility is measured with a susceptibility bridge (KLY-1) and combined with the anisotropy values. Both instruments use alternating current methods. Two series of measurements were performed with the spinner magnetometer (effective applied field: 0.246 mT at 10 kHz). Initially, the cylindrical sandstone samples were measured with the instrument in its commercial configuration. In a second measuring series, an accessory Krohn-Hite low-pass active filter (amplification: 20 dB; cut-off frequency: 16 kHz) was adapted to the instrument to improve its sensitivity and stability.

2. To determine magnetic anisotropy with the KLY-1 susceptibility bridge, the bulk susceptibility of cube-shaped samples is measured in 15 different positions according to Jelinek's (1973, 1977) measuring scheme. Again two measurement series were made. The first series was based on manual balancing of the bridge using its potentiometers, whereas the second series utilized the unbalanced output voltage of the bridge which then was connected on-line with the laboratory computer. In the latter configuration the instrumental noise is reduced appreciably by signal stacking and instrumental drift can be easily compensated for.

3. The ScT cryogenic magnetometer can be used to measure absolute susceptibilities by trapping a constant magnetic field in the instrument (applied field used in this study: 0.045 mT) during cooling through the superconducting critical point (Scriba and Heller, 1978). The total magnetization is recorded for nine positions, 45° apart, in each of three orthogonal planes. The signals are processed on-line so that the anisotropy ellipsoid can be calculated after subtraction of the remanence signal and correction for instrumental drift.

4. Finally, a set of 44 sandstone samples was measured after annealing at a temperature of 750° C, which had been observed to increase the low-field bulk susceptibility.

The results of the different measuring techniques are presented in Figs. 5–7 and Table 2. Figure 5 shows data from 69 sandstone samples measured (a) with the unmodified spinner magnetometer, (b) with this instrument utilizing the low-pass active filter and (c) with the cryogenic magnetometer. The susceptibility minima cluster very well around a direction nearly normal to bedding, as expected for a sedimentary fabric. When the mean direction of each principal anisotropy axis is calculated independently (although this is mathematically not strictly correct), small circular standard deviations (Table 2) result for the minimum axes. This is because the oblateness of the anisotropy ellipsoids is always strong with a 5%–7% degree of anisotropy between maximum and minimum susceptibility ($P_1$ factors in Table 2). The ratio of maximum to intermediate anisotropy axes ($P_2$), however, only rarely exceeds 1%. The

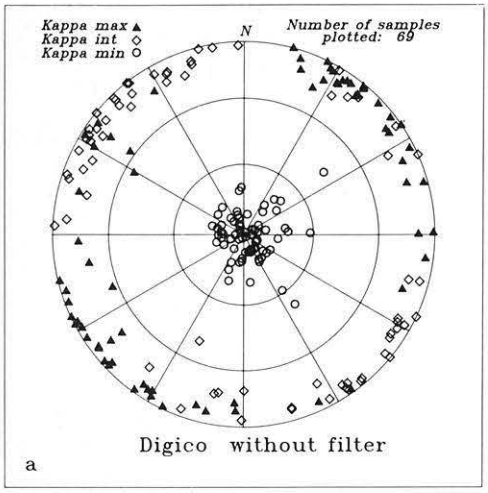


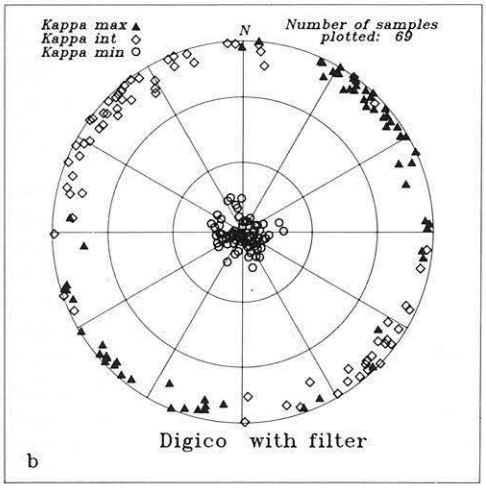


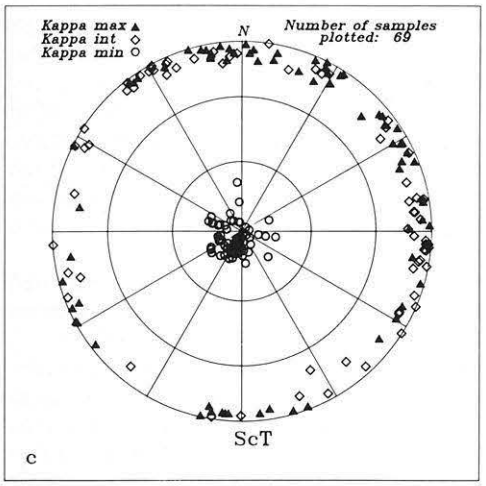


5

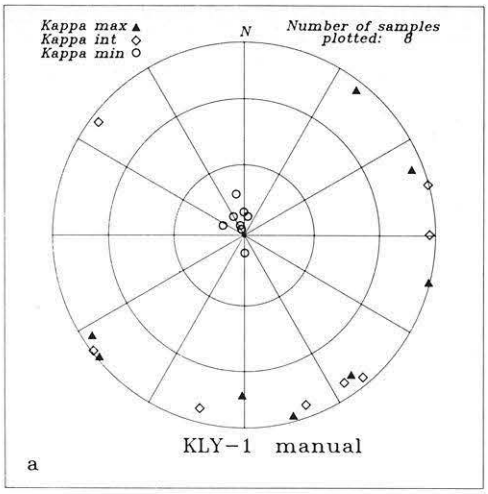


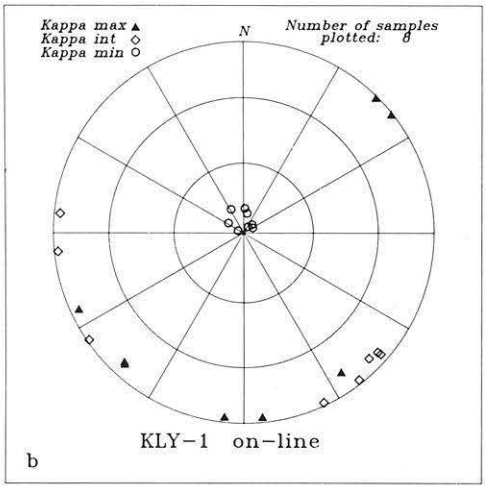


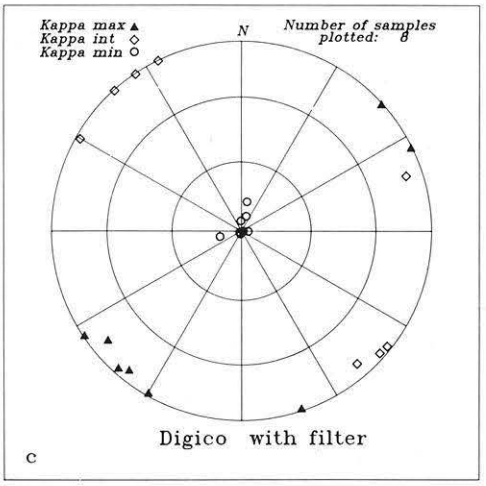


6

**Fig. 5a–c.** Anisotropy data measured **a** with the spinner magnetometer in its commercial configuration, **b** stabilized with a low-pass active filter and **c** with the cryogenic magnetometer. Most consistent data are obtained with the stabilized spinner magnetometer

**Fig. 6a–c.** Comparison of AC bridge and spinner magnetometer anisotropy results. **a** "manual", **b** "on-line" bridge measurements and **c** stabilized spinner magnetometer

directional scatter in the horizontal plane of the unfiltered Digico and the ScT measurements is high and the maximum axes are distributed along a great circle, with a slight preferred clustering about a NE-SW axis. Measurements with these techniques cannot be used to determine current directions in the sandstones with sufficient precision. Implementation of the low-pass active filter in the Digico spinner magnetometer lowers the instrumental noise level by a factor 10–100. This results in a distinct reduction of the scatter of the maximum susceptibility directions. Now they group

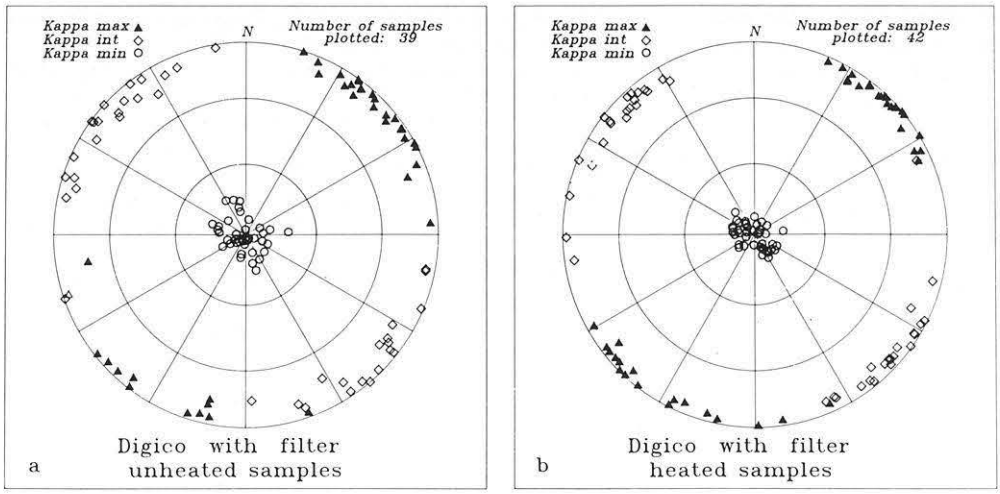


**Fig. 7a, b.** Anisotropy of **a** unheated and **b** heated sandstone samples measured with the stabilized spinner magnetometer

closely around an axis with mean azimuth of N47°E (S47°W).

Ten cube-shaped samples were measured on the susceptibility bridge and with the improved spinner magnetometer (Fig. 6). On both instruments two samples were discarded because the 95% confidence angle of the sample measurement of at least one axis (maximum or intermediate) exceeded the critical value for non-randomness (Jelinek, 1977). Even with this restriction, the manually adjusted bridge measurements of the maximum axes are highly scattered. When the bridge measurements are monitored on-line with the computer, more consistent data result which, however, are still of inferior quality compared to the actively filtered spinner magnetometer results. The minimum anisotropy directions are again well defined.

The most consistent anisotropy data were obtained on the stabilized spinner magnetometer from a set of 39 unheated samples and a sister set of 42 heated samples (Fig. 7) which gave individual measurements acceptable at the 95% confidence limit (Jelinek, 1977). In both data sets the directions of all three principal axes group well. The sedimentary fabric with very steeply inclined minimum directions is confirmed and the maximum axes group rather tigthly around a sub-horizontal NE-SW direction (Table 2). An up-current imbrication of the maximum axes was noted by Crimes and Oldershaw (1967) but cannot be discerned in the Plattensandstein. On the contrary, there are maximum axes clusters on both the NE and SW quadrants of the lower hemisphere projection, but with a tendency (2:1) to dip towards the NE along the main current direction suggesting a down-current imbrication of these axes. This is also reflected by the very steeply dipping individual minimum anisotropy axes which form a subvertical mean direction (Table 2). The minimum axes follow an elliptical distribution the long axis of which is oriented NW-SE. This distribution is very similar to that of the cross-bedding poles (Fig. 2a) and is caused by the symmetric cross-bedding stratification of the trough fillings (see Fig. 1). The magnetic low-field anisotropy of the Plattensandstein formation in this manner, reflects the original depositional fabric.

The heat treatment improves the quality of the anisotropy measurements. The mean susceptibility increases by about 300% and the degree of anisotropy rises sharply to 20% (Table 2). The resulting directional distribution of the maximum and intermediate anisotropy axes is very similar to that of the unheated samples but less scattered (Fig. 7b; Table 2). This improvement, however, can be achieved only with anisotropy meters using an alternating current method. The cryogenic magnetometer method, using a locked-in constant magnetic field, deteriorates because of a strong remanence viscosity originating from the superparamagnetic magnetite produced during the heating.

## Discussion and conclusion

The Plattensandstein sediments in the outcrop investigated have a clearly developed magnetic anisotropy. The minimum axes lie perpendicular to the bedding planes of the cross-bedded layers, thus indicating a sedimentary detritic fabric rather than a post-sedimentary compaction fabric. The differences between maximum and intermediate susceptibility axes are very small (below 1%) for the samples in the natural state. Their orientation can be resolved best by accurate measurements with the modified spinner magnetometer. This technique is also a very quick procedure since one sample can be measured within less than 1 min. Even higher accuracy is achieved by using heated sandstone samples which contain magnetite produced at high temperature. The magnetite fabric obviously mimics the natural pre-heating fabric, but can be measured more accurately due to the largely increased bulk susceptibility and its anisotropy.

Field-measurements of foresets yield a bimodal distribution (Fig. 2) which is caused by the symmetric filling from both sides of the cross-bedded structures. The resulting vector mean represents the main palaeocurrent direction. It points towards the NNE with an azimuth of $18.5° \pm 5.1°$ (circular standard error) and deviates by about 20° from the mean of the maximum susceptibility axes of the heated sandstones which is aligned parallel to a NE-SW axis with an azimuth of $38.5 \pm 3.0°$ or $218.5° \pm 3.0°$ (Fig. 7b). The azimuthal difference between these directions is significant, since their error cones do not overlap each other.

The magnetic determination of the palaeocurrent axial direction is more accurate than the result of the geological field observations. Since the mean of the susceptibility minima, however, is subvertical, up-stream or down-stream direction of the palaeocurrent cannot be discerned from the

present anisotropy measurements alone. Thus a combination of both geological field measurements, which resolve the trend of the transport direction, and precise measurements of the anisotropy principal directions gives the best estimate of the palaeocurrent directions in the sandstones of the Plattensandstein formation in southern Germany.

*Acknowledgements.* We thank H. Vossmerbäumer and K. Ernstson for critically reading the manuscript, W. Lowrie and R. Freeman for invaluable suggestions for improvement of the manuscript, M. Grieder for his help with the installation of the low pass filter and W. Gruber for sample preparation.

## References

Allen, J.R.L.: A review of the origin and characteristics of recent alluvial sediments. Sedimentology **5**, 89–191, 1965

Argenton, H., Bobier, C., Polveche, J.: La mesure de l'anisotropie de susceptibilité magnétique dans les flysches: application a la recherche des directions des paleocourrants. Sediment. Geol. **14**, 149–167, 1975

Bleil, U., Petersen, N.: Magnetic properties of minerals. In: Physical properties of rocks. G. Angenheister ed. pp 308–365 Springer: Berlin-Heidelberg-New York, 1982

Channell, J., Heller, F., Stuijvenberg, J. van: Magnetic susceptibility anisotropy as an indicator of sedimentary fabric in the Gurnigel Flysch. Eclog. Geol. Helv. **73**, 781–787, 1979

Collinson, D.W.: The origin of remanent magnetization and initial susceptibility of certain red sandstones. – Geophys. J. R. Astron. Soc. **9**, 203–217, 1965

Collinson, D.W.: Ferrous and ferric iron in red sediments and their magnetic properties. Geophys. J. R. Astron. Soc. **16**, 531–542, 1968

Crimes, T.P., Oldershaw, M.A.: Paleocurrent determinations by magnetic fabric measurements of the Cambrian rocks of St. Tudwal's Peninsula, North Wales. Geol. J. **5**, 217–232, 1967

Dunlop, D.J.: Magnetic mineralogy of unheated and heated red sediments by coercivity spectrum analysis. Geophys. J. R. Astron. Soc. **27**, 37–55, 1972

Fisher, R.A.: Dispersion on a sphere. Proc. Roy. Soc. London, **A 217,** 295–305, 1953

Galehouse, J.S.: A test of the method using the anisotropy of magnetic susceptibility as a paleocurrent indicator. Geol. Soc. Am. Bull. **79**, 387–390, 1968

Hamilton, N.: The effect of magnetic and hydrodynamic control on the susceptibility anisotropy of redeposited silt. J. Geol. **75**, 738–743, 1967

Hamilton, N., Rees, A.I.: The anisotropy of magnetic susceptibility of the Franciscan rocks of the Diablo Range, Central California. Geol. Rdsch. **60**, 1103–1124, 1971

Hamilton, N., Owens, W.H., Rees, A.I.: Laboratory experiments on the production of grain orientation in shearing sand. J. Geol. **76**, 465–472, 1968

Hrouda, F., Janak, F.: A study of the hematite fabric of some red sandstones on the basis of their magnetic susceptibility anisotropy. Sediment. Geol. **6**, 187–199, 1971

Ising, G.: On the magnetic properties of varved clay. Ark. Math. Astr. Phys. **29A**, 1–37, 1942

Jelinek, V.: Precision a.c. bridge set for measuring magnetic susceptibility of rocks and its anisotropy. Studia Geophys. Geod. **17**, 36–47, 1973

Jelinek, V.: The statistical theory of measuring anisotropy of magnetic susceptibility of rocks and its application. Geofyzika Brno, 88p, 1977

Rad, U. von: Comparison between "magnetic" and sedimentary fabric in graded and cross-laminated sand layers, Southern California. Geol. Rdsch. **60**, 331–354, 1970

Rees, A.I.: The effect of water currents on the magnetic remanence and anisotropy of susceptibility of some sediments. Geophys. J. R. Astron. Soc. **5**, 251, 1961

Rees, A.I.: The use of the anisotropy of magnetic susceptibility in the estimation of sedimentary fabric. Sedimentology **4**, 257–271, 1965

Rees, A.I.: The production of preferred orientation in a concentrated dispersion of elongated and flattened grains. J. Geol. **76**, 457–465, 1968

Rees, A.I., Rad, U. von, Shepard, F.P.: Magnetic fabric of sediments from the La Jolla submarine canyon and fan. Marine Geology **6**, 145–178, 1968

Scriba, H., Heller, F.: Measurements of anisotropy of magnetic susceptibility using inductive magnetometers. J. Geophys. **44**, 341–352, 1978

Shive, P.N., Steiner, M.B., Huycke, D.T.: Magnetostratigraphy, paleomagnetism, and remanence acquisition in the Triassic Chugwater formation of Wyoming. J. Geophys. Res. **89**, 1801–1815, 1984

Stephenson, A.: The effect of heat treatment on the magnetic properties of Old Red Sandstone. Geophys. J. R. Astron. Soc **13**, 425–440, 1967

Teyssen, T., Vossmerbäumer, H.: Schrägschichtungsanalyse am Beispiel des Buntsandsteins in Nordbayern. N. Jb. Geol. Paläont. Mh. **10**, 620–642, 1980

Turner, P: Continental red beds. Developments in Sedimentology, **29**, pp 1–562. Elsevier: Amsterdam, 1980

Van den Ende, C.: On the origin of anisotropy of magnetic susceptibility in the Permian red beds from the western parts of the Dôme de Barrot (S. France). In: Progress in geodynamics, Borradaile, G.J. et al. eds. Proc. Nat. Symp. Geodynamics. pp 176–189, 1975

Vossmerbäumer, H., Achtnich, T., Kistner, A., Priebe, H., Rongitsch, A., Rückert, E., Schultz, T., Teyssen, T.: Schüttungsrichtungen im Plattensandstein (Trias, Oberer Buntsandstein) Frankens. Geol Bl. NO-Bayern, **29**, 50–60, 1979

Wurster, P.: Geometrie und Geologie von Kreuzschichtungskörpern. Geol. Rdsch. **47**, 322–359, 1958

Received December 17, 1984; Revised February 4, 1985
Accepted February 4, 1985